HHS Public Access

Author manuscript

Hepatology. Author manuscript; available in PMC 2019 October 01.

Published in final edited form as:

Hepatology. 2018 October ; 68(4): 1347–1360. doi:10.1002/hep.29914.

NEUTROPHIL EXTRACELLULAR TRAPS PROMOTE INFLAMMATION AND DEVELOPMENT OF HEPATOCELLULAR CARCINOMA IN NON-ALCOHOLIC STEATOHEPATITIS

Dirk J. van der Windt[1,*], **Vikas Sud**[1,*], **Hongji Zhang**[1], **Patrick R. Varley**[1], **Julie Goswami**[1], **Hamza O. Yazdani**[1], **Samer Tohme**[1], **Patricia Loughran**[2], **Robert M. O'Doherty**[3], **Marta I. Minervini**[4], **Hai Huang**[1,5], **Richard L. Simmons**[1], and **Allan Tsung**[1]

[1]Department of Surgery, University of Pittsburgh Medical Center, Pittsburgh, Pennsylvania, USA

[2]Center for Biologic Imaging, Department of Cell Biology, University of Pittsburgh Medical Center, Pittsburgh, Pennsylvania, USA

[3]Division of Endocrinology and Metabolism, Department of Medicine, University of Pittsburgh, Pennsylvania, USA

[4]Department of Pathology, University of Pittsburgh Medical Center, Pittsburgh, Pennsylvania, USA

[5]Department of Surgery, Union Hospital, Huazhong University of Science and Technology, Wuhan, P.R. China

Abstract

Nonalcoholic steatohepatitis (NASH) is a progressive, inflammatory form of fatty liver disease. It is the most rapidly rising risk factor for the development of hepatocellular carcinoma (HCC), which can arise in NASH with or without cirrhosis. The inflammatory signals promoting the progression of NASH to HCC remain greatly unknown. The propensity of neutrophils to expel decondensed chromatin embedded with inflammatory proteins, known as neutrophil extracellular traps (NETs), has been shown to be important in chronic inflammatory conditions and in cancer progression. In this study, we asked whether NET formation occurs in NASH and contributes to the progression of HCC. We found elevated levels of a NET marker in serum of patients with NASH. In livers from STAM mice (NASH induced by neonatal streptozotocin and high fat diet), early neutrophil infiltration and NET formation was seen, and was followed by an influx of monocyte-derived macrophages, production of inflammatory cytokines, and progression of HCC. Inhibiting NET formation, through treatment with DNase or using mice knocked-out for peptidyl arginine deaminase type IV ($PAD4^{-/-}$), did not affect the development of a fatty liver, but altered the consequent pattern of liver inflammation, which ultimately resulted in decreased tumor growth.

Corresponding author contact information: Dr. Allan Tsung, MD, tsunga@upmc.edu, Telephone number: 412-692-2001, Fax number: 412-692-2002, Address: 3459 Fifth Avenue, UPMC Montefiore, 7 South, Pittsburgh, PA 15213-2582.
*These authors contributed equally to this work.

The authors declare that no conflict of interest exists

Author contributions

DJvdW, VS, ST, HH, RLS, and AT conceived the study, designed the experiments, interpreted the results, and wrote the manuscript. DJvdW, VS, PV, JG, HZ, HOZ, and ST performed the experiments. PL performed immunofluorescent staining and interpreted the images. RMOD designed the experiments and provided essential reagents. MIM performed pathologic analysis of liver samples. The authors thank Xinghua Liao and Heather Waring for excellent technical assistance.

Mechanistically, we found that commonly elevated free fatty acids stimulate NET formation in vitro.

Conclusion—Our findings implicate NETs in the protumorigenic inflammatory environment in NASH, suggesting that their elimination may reduce the progression of liver cancer in NASH.

Keywords

NASH; monocytes; inflammatory cytokines; cancer progression; free fatty acids

Introduction

As a result of its sharply increasing prevalence in western and non-western societies, non-alcoholic fatty liver disease (NAFLD) has become the most common chronic liver disease worldwide (1). In NAFLD, steatosis can progress to a chronic inflammatory condition (non-alcoholic steatohepatitis - NASH), which places patients at risk for developing cirrhosis, liver failure, and hepatocellular carcinoma (HCC) (2). A significant proportion of HCC in NASH occurs without cirrhosis as a required intermediate (3), underlining the importance of inflammation as a hallmark for cancer development and progression (4).

The pathophysiology of NASH is complex and incompletely understood. Besides genetic and molecular factors, innate immune activation has been essential for amplifying hepatic inflammation and progression to HCC (5). Neutrophils have long been noted in the inflammatory cell infiltrate of NASH (6), but little is known about their role in the disease process. Indeed, neutrophils are common infiltrating cells in almost every type of acute inflammation and a component of most chronic inflammatory infiltrates.

In 2004, Brinkman et al reported a previously undescribed property of neutrophils, i.e. that neutrophils can expel their nuclear material to establish neutrophil extracellular traps (NETs), which can entrap and kill bacteria (7). Soon thereafter, Buchanan et al demonstrated that DNase dissolved NETs and thereby eliminated their microbicidal properties (8). During the past decade, the importance of NETs in non-infectious inflammation has been discovered in chronic inflammatory conditions including atherosclerosis and rheumatoid arthritis (9). In addition, a growing body of evidence has emerged pointing to the promotion of cancer growth and proliferation by the appearance of NETs in the cancer inflammatory microenvironment (10). We have recently reported that NETs alter the inflammatory neutrophil-rich microenvironment associated with hepatic ischemic stress with the result that both the capture of circulating colon cancer cells and the growth of liver metastatic foci are facilitated in mice (11).

The role of NETs in NASH and its progression to HCC has not been thoroughly studied. The present experiments were designed to investigate the possible role of NETs in the evolution of NASH and its progression to HCC in a mouse model with clinical relevance. Blockade of NETs in a standard NASH model was found to modify the pattern of liver inflammation and inhibit the development of hepatocellular carcinoma.

Materials and Methods

Patient samples

Serum samples were collected pre-operatively from patients scheduled to undergo partial hepatectomy at the University of Pittsburgh (Pittsburgh, PA) between 2010 and 2017. Human studies were approved by the University of Pittsburgh Institutional Review Board (PRO08010372) and all patients signed informed consent. Pathologic analysis reports of resected liver specimens were reviewed to identify 56 patients with a histologic diagnosis of NASH. During the same time period, we identified 30 patients with normal background liver histology. Patients with liver fibrosis and chronic viral hepatitis were excluded from the analysis. Both groups were evaluated for baseline characteristics including age, gender and diagnosis (benign liver disease, primary hepatobiliary malignant disease, or metastatic disease to the liver). Using enzyme-linked immunosorbent assay (ELISA), serum levels of MPO–DNA complexes were measured for both groups and compared to MPO-DNA levels of healthy volunteers.

Animals and animal models

Animal protocols were approved by the Institutional Animal Care and Use Committee and adhered to the NIH Guidelines. Male and female C57BL/6J mice were purchased from Jackson Laboratories, Bar Harbor, USA. Peptidyl arginine deiminase type IV knockout ($PAD4^{-/-}$) mice were a gift from Dr. Yanming Wang, Pennsylvania State University, State College, PA. $LysM^{eGFP}$ knockin mice were a gift from Dr. Thomas Graf. We used the STAM model of NASH/HCC (12) in which mice are exposed to diabetes and high fat diet. Wild type C57BL/6J, $PAD4^{-/-}$ or $LysM^{eGFP}$ pups were injected intraperitoneally with 200μg of Streptozotocin (Sigma Aldrich) within 5d after birth, followed by feeding with 60% high-fat diet (HFD, Research Diets, D12492) ad libitum from the age of 3 weeks.

NET inhibition with DNase

To inhibit NET formation, we treated STAM mice with DNase (DNase I, Roche), starting at the day pups were weaned from their mothers at 3 weeks of age. Dosage was 50μg IP 3x/week, comparable to a regimen previously used to effectively block NET-macrophage interaction (13). For selected experiments DNase was administered daily.

Detection of NETs and NET-specific markers

Western blot assays were performed on whole cell lysates from mouse liver tissue. Membranes were incubated overnight with anti-citrullinated histone-3 (CitH3, 1:1000, Abcam) and anti-3-chlorotyrosine (1:500, Hycult) as a primary antibody, with anti-rabbit secondary antibody (1:10000). β-actin was used as an internal control. To quantify NETs in human serum, mouse serum, and cell culture supernatant, a capture ELISA to detect myeloperoxidase (MPO) associated with DNA (MPO-DNA) was performed as described previously (14). For the capture antibody, a human or mouse MPO ELISA kit (Hycult biotech, HK210-01) was used according to the manufacturer's directions. A peroxidase-labeled anti-DNA mAb (component No.2, Cell Death ELISAPLUS, Roche) was used. For immunohistochemistry studies, formalin fixed and paraffin embedded liver samples were

stained with anti-Ly6G (BD Pharmingen, clone 1A8) and anti-3-chlorotyrosine antibodies. For immunosfluorescent staining, LysM^{eGFP} livers were fixed in 4% paraformaldehyde and placed in 30% sucrose prior to sectioning. NETs were stained for with primary antibodies against CitH3 (5ug/mL, Abcam). DAPI (Sigma) and anti-actin antibody (Abcam) were used for nuclear and cell wall delineation, respectively. All slides were scanned under the same conditions for magnification, exposure time, lamp intensity and camera gain. Confocal images were acquired using Olympus Fluoview 1000 microscope with a PlanApo N (40x with and without a 2.5 digital zoom). Sequential scanning was applied for acquiring individual emission channels when multiple fluorophores were involved. The thickness of the sections were imaged by focusing on the top of the section, setting the Z-axis to 0, and then refocusing to the bottom of the section, an average of 8 sections were acquired.

Neutrophil isolation and in-vitro NET formation

The bone marrow of the femur and tibia were collected from WT mice as previously described by Cools-Lartigue et al (15). Neutrophils were sorted with a BD-Aria-Plus high-speed sorter using APC conjugated anti-CD11b monoclonal antibody and APC-Cy7 conjugated anti-Lys6G monoclonal antibody (both BD Pharmingen). 2×10^6 neutrophils were plated onto gelatin coated 6cm dishes and onto gelatin coated glass cover slips, and allowed to attach to the plate during a 1 hour incubation period at 37°C. The FFA palmitic (C16:0), linoleic (C18:2), and oleic acid (C18:1) (all from Nu-Check Prep) were dissolved in 25% FFA-free BSA and were added in a final concentration of 50uM to stimulate the neutrophils. LPS at 100nM and H_2O_2 (both Sigma) were used as positive controls, whereas 25% BSA without FFA served as negative control. After 4 hours of stimulation at 37°C, the supernatants were spun and frozen for analysis of MPO-DNA levels. Cover slips were stained with antibodies against histone 2AX (Abcam ab20669, with Alexa Fluor 555 goat anti-rabbit secondary antibody from Life Technologies), actin (Alexa Fluor 488, Invitrogen) and DAPI, and NET formation was visualized with an Olympus Fluoview 1000 microscopic camera.

Statistical analysis

Experimental results are expressed as mean ± SEM. Comparisons were performed using student's t-test and ANOVA. For the data analysis of human patients, the baseline characteristics for each group were compared using χ^2 test for categorical variables, and Mann Whitney test for continuous variables. MPO-DNA levels in human serum were compared using Mann Whitney and Kruskal Wallis nonparametric tests. For all analyses, a two-tailed p value <0.05 was considered statistically significant.

Additional methods can be found online in Supplementary Methods.

Results

NET marker MPO-DNA is elevated in patients with NASH

We analyzed preoperative serum samples, collected from patients undergoing partial hepatic resection at our institution, for MPO-DNA complexes. When neutrophils form NETs, chromatin DNA associated with other neutrophil proteins is released. By measuring MPO-

DNA complexes, we can be certain that the nucleosomes are derived from NET formation (14). Between 2010–2017, we identified 56 patients who underwent liver resection and had histologic evidence of NASH on pathologic examination of their resected specimen. These patients were matched for age and indication for liver resection to 30 patients with normal liver background on pathology. NASH patients had higher BMI, higher ALT levels and a higher rate of diabetes, whereas other characteristics were comparable between the two groups (Supporting Table S1). NASH patients had significantly higher levels of MPO-DNA levels in their preoperative serum, irrespective of the presence of either benign, primary malignant, or metastatic disease in the liver, compared to patients with normal liver (Fig. 1).

Neutrophils infiltrate murine NASH livers and undergo NET formation

To test our hypothesis that NETs promote inflammation in NASH, we utilized the STAM model of murine NASH. This model is characterized by its close resemblance to human NASH in male and female mice with consistent progression to HCC in male mice (12). The administration of streptozotocin to neonatal C57BL/6 mice followed by a high fat diet yielded mice with elevated blood glucose levels (546±26 mg/dL compared to 213±17 mg/dL in control mice) (Fig. 2A). STAM mice developed mildly increased serum ALT levels (Fig. 2B), and a gradual increase in liver weight averaging 1.6x the normal liver weight by 20 weeks (2.42±0.33 g vs. 1.52±0.07 g, p=0.04). Histopathologic staging by a blinded experienced liver pathologist showed early onset of a steatotic liver and a gradual increase in NAS to an average score of 6/8 by 20 weeks (Fig. 2C), whereas healthy control mice did not develop NASH (NAS 0 at all time points, not shown). HCC tumors began appearing in some mice by 16 weeks, with the surface of all male livers being studded with HCC by 20 weeks (Fig. 2D). We explored the phenotype of liver infiltrating innate immune cells with flow cytometric analysis of isolated non-parenchymal liver cells. The applied gating strategy is shown in Supporting Fig. S1. An influx of neutrophils in STAM livers started at 5 weeks, resulting in an approximately 2-fold increase (Fig. 3A and B). Western blot analysis revealed that CitH3, a specific marker of NET formation (16), was present in STAM livers. Although neutrophil numbers returned to baseline by 12 weeks, NET formation was persistently detectable for the 20 weeks duration of the experiment (Fig. 3C). In search for further evidence of NET formation in NASH, we exposed LysM-GFP knock-in mice to the STAM model of NASH. This gene mutation causes the expression of GFP on myeloid immune cells, which we visualized on liver sections with concomitant immunofluorescent staining for CitH3. In livers from STAM mice, GFP/CitH3-positive infiltrates including cells with clear NET morphology were detectable from the age of 6 weeks (Fig. 3D).

NET formation is followed by monocyte infiltration and inflammatory cytokine production

Because LysM expression is not limited to neutrophils but is also present on other cell types of myeloid origin, we compared the expression of GFP on neutrophils, infiltrating macrophages and Kupffer cells. GFP expression on liver neutrophils was 10x higher than on infiltrating macrophages and 3 log higher than on Kupffer cells (Supporting Fig. S2), indicating that neutrophils are the most likely source of the observed GFP signal. In particular, the early neutrophil recruitment, GFP-positive cell infiltration, and NET formation were followed by a population of infiltrating macrophages derived from monocytes (Fig. 3E). These cells are characterized by $CD45^{+}CD11b^{+}F4/80^{low}$ surface

staining and are variable in their expression of Ly6C, an inflammatory pattern previously described by other investigators (17, 18) (Supporting Fig. S1). In contrast to Kupffer cells, the resident macrophages of the liver, infiltrating macrophages arise from monocytes that are being recruited to the liver in response to inflammation (18). They have been found to be predominant effector immune cells in NASH, and are a major source of inflammatory cytokines leading to amplification of the inflammation (19). The increase in infiltrating macrophages started only after the influx of neutrophils: Indeed, increased levels of the inflammatory cytokines IL-6 and TNF-α were only found after 8 weeks, when infiltrating macrophages became numerous (Fig. 3F and Supporting Fig. S3). By contrast, endogenous liver Kupffer cells ($CD45^{+}CD11b^{+}F4/80^{hi}$) followed a pattern of early depletion, likely followed by replacement by infiltrating macrophages that reached its maximum by 8 weeks of age (Supporting Fig. S4), as previously described (17).

NET inhibition reduces monocyte infiltration and inflammation

After confirming that NETs are formed in experimental NASH, we sought to investigate their contributory role in the evolution of the pattern of inflammation within the liver with a focus on the recruitment of infiltrating macrophages. To investigate this interaction, we applied two proven strategies to block NETs, being the use of $PAD4^{-/-}$ mice and the injection of DNase (11, 20). $PAD4^{-/-}$ mice are genetically deficient for PAD4, an enzyme that catalyzes the citrullination of histone 3, a critical step for the decondensation and expulsion of chromatin that is characteristic of NET formation (21). $PAD4^{-/-}$ mice are therefore naturally NET-deficient. DNase (50ug IP, administered three times weekly) resulted in the expected reduction of citH3 on western blot analysis of livers from STAM mice, demonstrating the efficacy of DNase to eliminate NETs (Fig. 4A). It also reduced the neutrophil infiltration into the liver (Fig. 4B). With immunohistochemistry for the location of neutrophils, it was found that DNase treatment greatly reduced the presence of neutrophils in the hepatic lobule indicating that DNase potentially reduces the extravasation of neutrophils from the sinusoids and their infiltration into the liver lobule (Supporting Fig. S5). Importantly, both DNase and $PAD4^{-/-}$ significantly changed the pattern of the liver inflammation by reducing monocyte-derived macrophage infiltration at 8 weeks, consistent with the idea that infiltrating macrophages were a partial consequence of NET formation (Fig. 4C). With NET blockade, IL-6 levels were reduced to baseline levels, concurrent with the decrease in infiltrating macrophages (Fig. 4D). Reductions in TNF-α mRNA levels in liver tissue homogenates (Fig. 4D) and serum ALT levels (Supporting Fig. S6), were also seen in NET-deficient STAM mice although comparisons did not reach statistical significance. To provide further evidence that NETs carry responsibility for the pathobiology of NASH, the effect of DNase on the formation of 3-chlorotyrosine adducts, previously shown to be a result of NET-specific oxidative damage (22), was investigated. DNase was found to reduce the increased 3-chlorotyrosine levels in livers of STAM mice (Supporting Fig. S7). The cumulative effect of the changes in hepatic inflammation by DNase was a decrease in NAS from 3.25±0.5 to 1.8±0.4, $p<0.05$ (Fig. 4E). When component scores of the NAS were compared, it was evident that the reduction in NAS was the result of a decrease in inflammation and ballooning, but that NET blockade did not affect steatosis (Fig. 4F). Despite lower levels of all other inflammatory markers, $PAD4^{-/-}$ unexpectedly did not reduce the NAS (Fig. 4E). As with DNase, a decrease in the score for inflammation was seen

(Fig. 4F), but steatosis and ballooning were increased in PAD4$^{-/-}$ mice, leading to an overall lack of reduction in NAS.

NET inhibition reduces progression of NASH to liver cancer

To investigate the long-term effect of NET blockade on the progression of NASH to HCC, we extended the treatment with DNase to the full 20 week time course of the experiments. In the shorter-term experiments discussed above both male and female mice were included, as they did not significantly differ in levels of inflammatory markers. However, for long-term experiments only male mice were used since, as previously described, only male STAM mice develop multiple liver tumors resembling HCC (12). When DNase was dosed 3x/week, tumor formation as evaluated by the number of liver surface tumors was reduced in approximately 50% of male mice (data not shown). However, when DNase dosage was increased to 50μg daily for 20 weeks, DNase-treated STAM mice developed only 1.3±1.1 surface tumors compared to 8.7±3.4 tumors in untreated co-housed STAM littermates ($p=0.001$) (Fig. 5A). Just as with DNase treatment, numbers of tumors counted on the liver surface were significantly reduced in PAD4$^{-/-}$ STAM mice compared to wild-type STAM mice (Fig. 5A). Tumors were also significantly smaller in DNase and PAD4$^{-/-}$ groups (Fig. 5B). Both applied strategies of NET inhibition seemed to persistently alter the inflammatory environment that gives rise to HCC in the NASH liver, with reduced IL-6 levels even after 20 week of exposure to the STAM model (Fig. 5C).

Commonly elevated free fatty acids in NASH stimulate NET formation in vitro

To investigate what a stimulus for NET formation in NASH could be, we investigated the role of FFA, as FFA are considered the link between excess liver fat and the activation of various inflammatory pathways in NASH (23). First, we confirmed the increased presence of free fatty acids in the livers of STAM mice. Similar to the non-reduced degree of steatosis on histology, NET abrogation with DNase and PAD4$^{-/-}$ neither changed the elevated level of FFA in NASH livers, nor the elevated levels of serum triglycerides (Fig. 6A and 6B). We then stimulated neutrophils isolated from mouse bone marrow with the 3 FFA that are most significantly elevated in livers affected by NASH, being palmitic (C16:0), linoleic (C18:2), and oleic acid (C18:1) (24). Palmitic and linoleic acid were found to be able to induce NET formation to a similar extent as LPS, as measured by MPO-DNA complexes in culture supernatants (Fig. 6C). Immunofluorescent imaging showed a pattern of NET formation concordant with MPO-DNA levels (Fig. 6D), namely that NETosis (equivalent to that produced by hydrogen peroxide) resulted from the exposure of neutrophils to linoleic and palmitic acid, but not to oleic acid.

Discussion

NAFLD and NASH affect a significant proportion of the western population and form a spreading epidemic to developing countries (1). A concerning observation is the relatively high incidence of HCC in NASH before the development of cirrhosis (3). This observation emphasizes the important role of inflammation in cancer development and progression in NASH. The inflammatory signals that facilitate this pathobiology are still greatly unknown. In this study, we show that in NASH neutrophils are stimulated to form NETs, and that

inhibition of NETosis significantly reduced the presence of infiltrating macrophages, the production of inflammatory cytokines, and the development of HCC in a clinically relevant mouse model of NASH.

We began our investigation with the evaluation of human serum samples for the NET marker MPO-DNA and found that MPO-DNA levels were significantly elevated in patients in whom their resected liver specimen had histologic evidence of NASH, compared with patients with normal background liver histology. Stratification by indication for liver resection revealed that the presence of NASH was most likely responsible for this elevation in MPO-DNA, rather than the presence of benign vs. primary malignant vs. metastatic disease in the liver. Although this crude analysis does not account for other factors that may be of influence, such as the effect of preoperative chemotherapy on the liver, it provided support for the hypothesis that NET formation occurs in the inflammatory environment in NASH. NETs are extracellular, web-like structures of decondensed chromatin decorated with cytosolic and granule proteins (7), which have been shown to aid in the defense against bacteria, fungi, viruses, and parasites (25). However, if dysregulated, NETs can cause tissue damage and contribute to the pathogenesis of immune-related diseases, such as vasculitis, rheumatoid arthritis, and systemic lupus erythematosus (25). We have previously investigated NETs in the setting of acute sterile inflammation of the liver, and shown that elimination of NETs reduces ischemia and reperfusion injury favorable for the growth of metastatic deposits of colon cancer (11). NETosis has now been described to have a role in many non-infectious inflammatory conditions including diabetes, atherosclerosis, wound healing, as well as tumor growth (9). In NASH, the increased presence of neutrophils has been demonstrated (26), but to our knowledge this is the first study evaluating the role of NETs in NASH, an increasingly prevalent chronic inflammatory condition, which predisposes to HCC.

After verifying that NETs are also formed in an experimental mouse model of NASH, we sought to investigate their contributory role in the pathogenesis of this disease. Mice developed fatty livers irrespective of the presence or absence of NETs, which led to the hypothesis that NETs are formed as a consequence of increased liver fat and may be important in the evolution of the pattern of inflammation in the liver that progresses from steatosis to NASH. We focused our investigations on the relation between NETs and the recruitment of infiltrating macrophages, as these cells have been found to be predominant effector immune cells in NASH (19). Infiltrating macrophages arise from monocytes that are being recruited to the liver in response to inflammation (18), and have been reported to be a major source of inflammatory cytokines leading to amplification of the inflammation (19). Neutrophil-monocyte/macrophage interactions have previously been shown to be crucial for NASH development (27), and in different chronic inflammatory conditions such as atherosclerosis, recent work uncovered that this cross-talk can be facilitated by NETs (13). However, in NASH, a role of NETs in neutrophil-monocyte/macrophage interactions had thus far not been established. In STAM mice, we found that neutrophil infiltration and NET formation occurred early in the development of NASH. The increase in infiltrating macrophages started only after the influx of neutrophils. Indeed, increased levels of the inflammatory cytokines IL-6 and TNF-α were only found after 8 weeks, when infiltrating macrophages became numerous. Although the signaling pathways by which NETs attract

macrophages remain unknown in our work as well as in investigations by others (13), NET blockade significantly changed the pattern of the liver inflammation by reducing monocyte-derived macrophage infiltration, consistent with the idea that infiltrating macrophages were a consequence of NET formation. NET inhibition also reduced neutrophil infiltration itself, which is concordant with previous literature that NETs have a positive chemoattractive effect on the infiltration of more neutrophils (28).

With the use of LysM^{eGFP} mice, we visualized inflammatory cell infiltration during various stages of NASH development. Although LysM expression is not limited to neutrophils but is also present on other cell types of myeloid origin, we concluded that neutrophils are the most likely source of the observed GFP signal, as the expression of GFP on neutrophils was 10x higher than on infiltrating macrophages and 3 log higher than on Kupffer cells. In addition, the presence of GFP positive infiltrates as early as 6 weeks was concordant with the timing of neutrophil infiltration by flow cytometry and NET formation by both western blotting and immunofluorescence.

Taken together, our data are consistent with the idea that fat accumulation in hepatocytes is not dependent on NET formation, but that NET formation is an initiating event in the pathogenesis of full blown NASH, by regulating the inflammatory environment through the attraction of new monocyte-derived macrophages, a known effector cell in NASH progression. Inhibition of NETosis significantly reduces the presence of infiltrating macrophages, the production of inflammatory cytokines, and a reduction in NAS via improvements in hepatocyte ballooning and presence of inflammation on histologic analysis at 8 weeks. Although over time the cellular inflammation evolved, including a subsequent decline in neutrophils in the liver, NET formation was detectable throughout the course of the experiment. In line with our previous observations that continued NET generation facilitates the outgrowth of colorectal liver metastases (11), our current data are consistent with the idea that the chronic inflammatory microenvironment in the NASH liver enables the persistent formation of NETs that facilitate the accelerated growth of HCC to become evident by 20 weeks. In the long-term, NET elimination and the alterations in the inflammatory environment led to a reduction in progression to HCC. DNase and PAD4$^{-/-}$ were equally effective in reducing the development of HCC in STAM mice, confirming that the anti-tumor effect of DNase is mediated through blockade of NET formation. Our data support the hypothesis that NETs are critical to the creation of a chronic inflammatory liver microenvironment in NASH that is favorable to the development of HCC.

The role of NETs in cancer has been a topic of investigation since NETs were first noted in the tumor environment of pediatric patients suffering from Ewing sarcoma (29). In an experimental setting, an important role for NETs in cancer progression has been previously demonstrated in models of injected tumor cells simulating metastatic disease. In those models, an additional inflammatory stimulus for NETosis, such as the induction of sepsis (15), the injection of granulocyte colony-stimulating factor (30), or liver ischemia-reperfusion was applied (11). In a model of spontaneous small intestinal cancer, a role for NETs induced by thrombosis was shown, although direct NET inhibition was not investigated (31). In this work, we present novel evidence that NET formation in a chronic inflammatory process contributes to the development of a primary malignancy, and that

modulation of the inflammation with NET inhibition is able to effectively reduce progression of NASH to HCC. It is not yet clear, however, if genetic alterations required for HCC development are directly induced by NETs, or by components of the subsequent inflammatory cascade. Recently, great progress has been made in the genetic analysis of HCC. However, there is no known signature of mutations in HCC in NASH (32).

We sought to further evaluate the conditions under which NASH induces infiltrating neutrophils to form NETs. We focused on free fatty acids (FFA) as a stimulus for augmented NET formation in the fatty liver, as FFA have been considered to be responsible for lipotoxicity in NASH (23). FFA are elevated in serum and livers of patients with fatty liver disease (24, 33, 34), as well as in the livers of mice in experimental models of NASH (35). In addition to having an effect on hepatocytes (36), FFA have recently been shown to have a toxic effect on CD4+ T cells in experimental NASH (37). However, the effects of FFA on neutrophils were unknown. First we noticed that NET abrogation with DNase and $PAD4^{-/-}$ did not reduce the level of steatosis. In fact, the absence of PAD4 seemed to increase the hepatocytes' susceptibility to non-inflammatory fatty changes when exposed to diabetes and high fat diet. We think this potentially indicates a hitherto unknown metabolic difference in $PAD4^{-/-}$ that has become the topic of our current ongoing investigations. NET inhibition also did not affect the level of FFA in the liver of STAM mice. Taken together, this suggests that NETs are not responsible for fat accumulation in the liver, but rather could be a consequence thereof. We then exposed isolated neutrophils to the FFA that were found to be most increased (10–25x higher than in healthy liver) in human NASH (24). Our experiments generated the first evidence known to us of the ability of FFA to induce neutrophils to form NETs. Although our experiments do not investigate for example the composition of FFA, which has previously been shown to be important for lipotoxicity (23), they reveal that some of the FFA most commonly elevated in NAFLD are a potential stimulus for NET-mediated inflammation in NASH. Previously, other investigators have shown that hyperglycemia can make neutrophils susceptible to undergo NETosis, but a second stimulus, e.g. LPS, was necessary to actually induce NETs in glucose-primed neutrophils (30). We hypothesize that in NASH, which often presents in the setting of metabolic syndrome including diabetes, hyperglycemia and FFA can synergize to prime and stimulate neutrophils to for NETs, which favor a protumorigenic environment.

It should be noted that in clinical NAFLD, only a subset of patients progresses to NASH, and an even smaller subset develops HCC. Although in clinical association studies, several risk factors for disease progression have been elucidated, including obesity, diabetes, age, and presence of advanced fibrosis or cirrhosis (38), the pathobiology remains greatly unknown. One explanation can be that the progression of NASH to HCC and cirrhosis is slower than in other etiologies of liver disease (39), preventing patients from developing these endpoints during their life span. The STAM model of accelerated progression of NAFLD to NASH/HCC provides opportunities to unravel the relation between NASH inflammation and cancer development.

In conclusion, our work provides evidence that NET formation plays an important role in the transition of steatosis to NASH. Blocking NETs did not affect steatosis and FFA accumulation in the liver, but prevented macrophage infiltration and changed the

inflammatory environment to one less favorable to HCC growth. Human patients with histologically proven NASH had increased serum levels of a known NET marker, indicating the clinical relevance of our findings. Strategies to eliminate NETs could be of great value in reducing the risk of HCC in fatty liver disease, which is among the most feared health epidemics predicted to occur in the upcoming decades, and is the only tumor of all common cancers in the US that has an increasing mortality (40).

Supplementary Material

Refer to Web version on PubMed Central for supplementary material.

Acknowledgments

Financial Support

This study was funded by NIH grants T32 AI 74490 (DJvdW), R01-GM95566 (AT), and 1S10OD019973-01 (Center of Biologic Imaging), by the Community Liver Alliance (AT), and by the National Natural Science Foundation of China Grant Number 81470902 (HH). This work benefitted from SPECIAL BD LSRFORTESSATM funded by NIH 1S10OD011925-01.

Abbreviations

ALT	alanine aminotransferase
CitH3	citrullinated histone-3
FFA	free fatty acids
HCC	hepatocellular carcinoma
NAFLD	non-alcoholic fatty liver disease
NAS	NASH activity score
NASH	nonalcoholic steatohepatitis
NET(s)	neutrophil extracellular trap(s)
NPC	nonparenchymal cells
PAD4	peptidyl arginine deaminase IV

References

Author names in bold designate shared co-first authorship.

1. Loomba R, Sanyal AJ. The global NAFLD epidemic. Nat Rev Gastroenterol Hepatol. 2013; 10:686–690. [PubMed: 24042449]
2. Wong VW, Chitturi S, Wong GL, Yu J, Chan HL, Farrell GC. Pathogenesis and novel treatment options for non-alcoholic steatohepatitis. Lancet Gastroenterol Hepatol. 2016; 1:56–67. [PubMed: 28404113]
3. Mittal S, El-Serag HB, Sada YH, Kanwal F, Duan Z, Temple S, May SB, et al. Hepatocellular Carcinoma in the Absence of Cirrhosis in United States Veterans is Associated With Nonalcoholic Fatty Liver Disease. Clin Gastroenterol Hepatol. 2016; 14:124–131. e121. [PubMed: 26196445]

4. Hanahan D, Weinberg RA. Hallmarks of cancer: the next generation. Cell. 2011; 144:646–674. [PubMed: 21376230]
5. Gao B, Tsukamoto H. Inflammation in Alcoholic and Nonalcoholic Fatty Liver Disease: Friend or Foe? Gastroenterology. 2016; 150:1704–1709. [PubMed: 26826669]
6. Ludwig J, Viggiano TR, McGill DB, Oh BJ. Nonalcoholic steatohepatitis: Mayo Clinic experiences with a hitherto unnamed disease. Mayo Clin Proc. 1980; 55:434–438. [PubMed: 7382552]
7. Brinkmann V, Reichard U, Goosmann C, Fauler B, Uhlemann Y, Weiss DS, Weinrauch Y, et al. Neutrophil extracellular traps kill bacteria. Science. 2004; 303:1532–1535. [PubMed: 15001782]
8. Buchanan JT, Simpson AJ, Aziz RK, Liu GY, Kristian SA, Kotb M, Feramisco J, et al. DNase expression allows the pathogen group A Streptococcus to escape killing in neutrophil extracellular traps. Curr Biol. 2006; 16:396–400. [PubMed: 16488874]
9. Jorch SK, Kubes P. An emerging role for neutrophil extracellular traps in noninfectious disease. Nat Med. 2017; 23:279–287. [PubMed: 28267716]
10. Erpenbeck L, Schon MP. Neutrophil extracellular traps: protagonists of cancer progression? Oncogene. 2017; 36:2483–2490. [PubMed: 27941879]
11. Tohme S, Yazadani HO, Al-Khafaji AB, Chidi AP, Lougharn P, Mowen K, Wang Y, et al. Neutrophil Extracellular Traps Promote the Development and Progression of Liver Metastases after Surgical Stress. Cancer Res. 2016; 76:1367–1380. [PubMed: 26759232]
12. Fujii M, Shibazaki Y, Wakamatsu K, Honda Y, Kawauchi Y, Suzuki K, Arumugam S, et al. A murine model for non-alcoholic steatohepatitis showing evidence of association between diabetes and hepatocellular carcinoma. Med Mol Morphol. 2013; 46:141–152. [PubMed: 23430399]
13. Warnatsch A, Ioannou M, Wang Q, Papayannopoulos V. Inflammation. Neutrophil extracellular traps license macrophages for cytokine production in atherosclerosis. Science. 2015; 349:316–320. [PubMed: 26185250]
14. Kessenbrock K, Krumbholz M, Schonermarck U, Back W, Gross WL, Werb Z, Grone HJ, et al. Netting neutrophils in autoimmune small-vessel vasculitis. Nat Med. 2009; 15:623–625. [PubMed: 19448636]
15. Cools-Lartigue J, Spicer J, McDonald B, Gowing S, Chow S, Giannias B, Bourdeau F, et al. Neutrophil extracellular traps sequester circulating tumor cells and promote metastasis. J Clin Invest. 2013
16. Leshner M, Wang S, Lewis C, Zheng H, Chen XA, Santy L, Wang Y. PAD4 mediated histone hypercitrullination induces heterochromatin decondensation and chromatin unfolding to form neutrophil extracellular trap-like structures. Front Immunol. 2012; 3:307. [PubMed: 23060885]
17. Reid DT, Reyes JL, McDonald BA, Vo T, Reimer RA, Eksteen B. Kupffer Cells Undergo Fundamental Changes during the Development of Experimental NASH and Are Critical in Initiating Liver Damage and Inflammation. PLoS One. 2016; 11:e0159524. [PubMed: 27454866]
18. Krenkel O, Tacke F. Liver macrophages in tissue homeostasis and disease. Nat Rev Immunol. 2017; 17:306–321. [PubMed: 28317925]
19. Baeck C, Wehr A, Karlmark KR, Heymann F, Vucur M, Gassler N, Huss S, et al. Pharmacological inhibition of the chemokine CCL2 (MCP-1) diminishes liver macrophage infiltration and steatohepatitis in chronic hepatic injury. Gut. 2012; 61:416–426. [PubMed: 21813474]
20. Huang H, Tohme S, Al-Khafaji AB, Tai S, Loughran P, Chen L, Wang S, et al. Damage-associated molecular pattern-activated neutrophil extracellular trap exacerbates sterile inflammatory liver injury. Hepatology. 2015; 62:600–614. [PubMed: 25855125]
21. Hemmers S, Teijaro JR, Arandjelovic S, Mowen KA. PAD4-mediated neutrophil extracellular trap formation is not required for immunity against influenza infection. PLoS One. 2011; 6:e22043. [PubMed: 21779371]
22. Smith CK, Vivekanandan-Giri A, Tang C, Knight JS, Mathew A, Padilla RL, Gillespie BW, et al. Neutrophil extracellular trap-derived enzymes oxidize high-density lipoprotein: an additional proatherogenic mechanism in systemic lupus erythematosus. Arthritis Rheumatol. 2014; 66:2532–2544. [PubMed: 24838349]
23. Alkhouri N, Dixon LJ, Feldstein AE. Lipotoxicity in nonalcoholic fatty liver disease: not all lipids are created equal. Expert Rev Gastroenterol Hepatol. 2009; 3:445–451. [PubMed: 19673631]

24. Yamada K, Mizukoshi E, Sunagozaka H, Arai K, Yamashita T, Takeshita Y, Misu H, et al. Characteristics of hepatic fatty acid compositions in patients with nonalcoholic steatohepatitis. Liver Int. 2015; 35:582–590. [PubMed: 25219574]
25. Papayannopoulos V. Neutrophil extracellular traps in immunity and disease. Nat Rev Immunol. 2017
26. Rensen SS, Slaats Y, Nijhuis J, Jans A, Bieghs V, Driessen A, Malle E, et al. Increased hepatic myeloperoxidase activity in obese subjects with nonalcoholic steatohepatitis. Am J Pathol. 2009; 175:1473–1482. [PubMed: 19729473]
27. Ye D, Yang K, Zang S, Lin Z, Chau HT, Wang Y, Zhang J, et al. Lipocalin-2 mediates non-alcoholic steatohepatitis by promoting neutrophil-macrophage crosstalk via the induction of CXCR2. J Hepatol. 2016; 65:988–997. [PubMed: 27266617]
28. Nemeth T, Mocsai A. Feedback Amplification of Neutrophil Function. Trends Immunol. 2016; 37:412–424. [PubMed: 27157638]
29. Berger-Achituv S, Brinkmann V, Abed UA, Kuhn LI, Ben-Ezra J, Elhasid R, Zychlinsky A. A proposed role for neutrophil extracellular traps in cancer immunoediting. Front Immunol. 2013; 4:48. [PubMed: 23508552]
30. Demers M, Wong SL, Martinod K, Gallant M, Cabral JE, Wang Y, Wagner DD. Priming of neutrophils toward NETosis promotes tumor growth. Oncoimmunology. 2016; 5:e1134073. [PubMed: 27467952]
31. Guglietta S, Chiavelli A, Zagato E, Krieg C, Gandini S, Ravenda PS, Bazolli B, et al. Coagulation induced by C3aR-dependent NETosis drives protumorigenic neutrophils during small intestinal tumorigenesis. Nat Commun. 2016; 7:11037. [PubMed: 26996437]
32. Zucman-Rossi J, Villanueva A, Nault JC, Llovet JM. Genetic Landscape and Biomarkers of Hepatocellular Carcinoma. Gastroenterology. 2015; 149:1226–1239. e1224. [PubMed: 26099527]
33. Zhang J, Zhao Y, Xu C, Hong Y, Lu H, Wu J, Chen Y. Association between serum free fatty acid levels and nonalcoholic fatty liver disease: a cross-sectional study. Sci Rep. 2014; 4:5832. [PubMed: 25060337]
34. Gambino R, Bugianesi E, Rosso C, Mezzabotta L, Pinach S, Alemanno N, Saba F, et al. Different Serum Free Fatty Acid Profiles in NAFLD Subjects and Healthy Controls after Oral Fat Load. Int J Mol Sci. 2016; 17:479. [PubMed: 27043543]
35. Larter CZ, Yeh MM, Haigh WG, Williams J, Brown S, Bell-Anderson KS, Lee SP, et al. Hepatic free fatty acids accumulate in experimental steatohepatitis: role of adaptive pathways. J Hepatol. 2008; 48:638–647. [PubMed: 18280001]
36. Feldstein AE, Werneburg NW, Canbay A, Guicciardi ME, Bronk SF, Rydzewski R, Burgart LJ, et al. Free fatty acids promote hepatic lipotoxicity by stimulating TNF-alpha expression via a lysosomal pathway. Hepatology. 2004; 40:185–194. [PubMed: 15239102]
37. Ma C, Kesarwala AH, Eggert T, Medina-Echeverz J, Kleiner DE, Jin P, Stroncek DF, et al. NAFLD causes selective CD4(+) T lymphocyte loss and promotes hepatocarcinogenesis. Nature. 2016; 531:253–257. [PubMed: 26934227]
38. Starley BQ, Calcagno CJ, Harrison SA. Nonalcoholic fatty liver disease and hepatocellular carcinoma: a weighty connection. Hepatology. 2010; 51:1820–1832. [PubMed: 20432259]
39. Pais R, Barritt ASt, Calmus Y, Scatton O, Runge T, Lebray P, Poynard T, et al. NAFLD and liver transplantation: Current burden and expected challenges. J Hepatol. 2016; 65:1245–1257. [PubMed: 27486010]
40. Ryerson AB, Eheman CR, Altekruse SF, Ward JW, Jemal A, Sherman RL, Henley SJ, et al. Annual Report to the Nation on the Status of Cancer, 1975–2012, featuring the increasing incidence of liver cancer. Cancer. 2016; 122:1312–1337. [PubMed: 26959385]

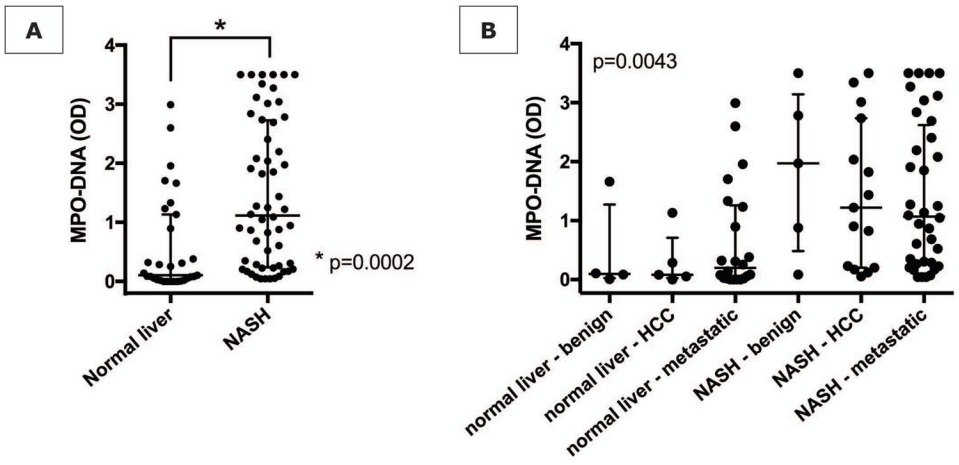

Figure 1. Increased NET marker in human NASH

(A) Patients with histopathologically proven NASH (n=46) have increased serum levels of MPO-DNA when compared with matched patients with normal liver histology (n=30). **(B)** MPO-DNA levels stratified by disease type (benign, primary malignant, metastatic). For any disease type, median MPO-DNA levels were higher when NASH was present in the background liver compared to a normal background liver.

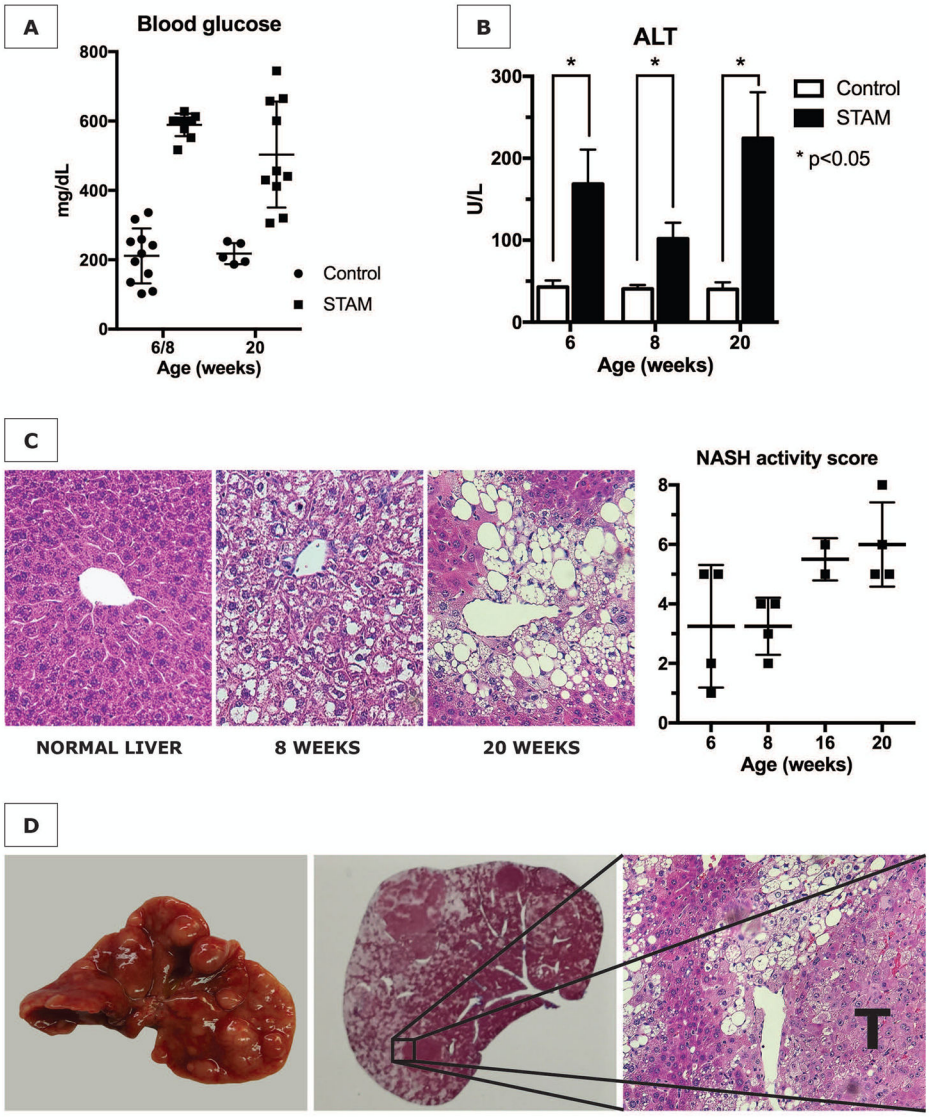

Figure 2. The STAM model of diabetes and high fat diet leading to NASH and HCC

(A) STAM mice are consistently hyperglycemic, **(B)** have elevated serum alanine aminotransferase (ALT) levels, and **(C)** develop steatosis with progressively increasing NASH activity scores (NAS). **(D)** By 20 weeks, male mice develop numerous liver tumors (T) with characteristics of hepatocellular carcinoma in the fatty liver background.

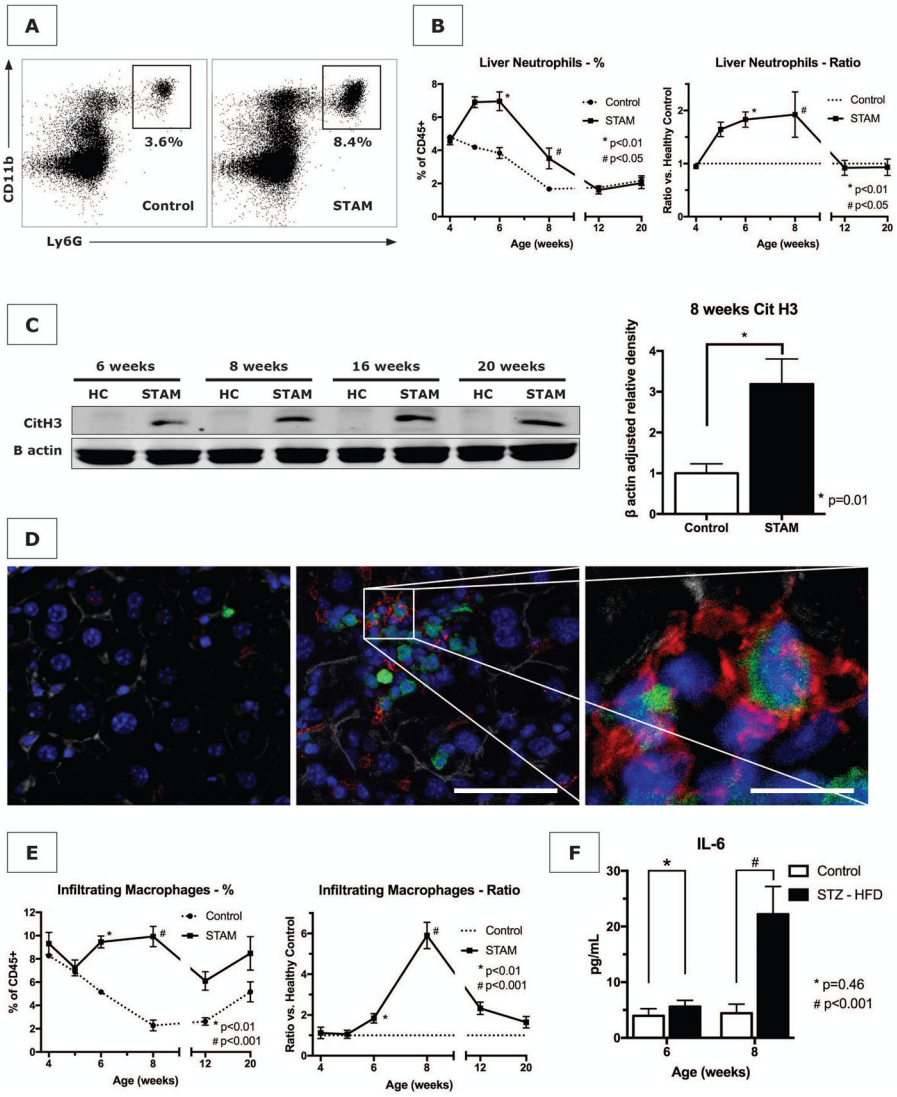

Figure 3. The STAM model of NASH results in neutrophil infiltration and NET formation prior to attraction of macrophages

(A and B) STAM mice demonstrate an increase in infiltrating neutrophils between 5 and 12 weeks in the liver starting at 5 weeks. Because healthy control mice demonstrated a decline in hepatic neutrophils during the first 2 months of life, neutrophil count can be expressed as a ratio of STAM/control mice. **(C)** Western blot of livers from STAM mice have elevated levels of the NET marker citrullinated histone 3 (CitH3), compared to age-matched healthy controls (HC), which persists throughout the full course of the experiment. On quantification for age 8 weeks (n=4 in each group), CitH3 was significantly increased in STAM mice. **(D)** By 6 weeks of age, GFP-positive infiltrates (green) are detectable in STAM livers (middle panel, scale bar 100μm), compared to healthy control in left panel, with abundant presence of CitH3 immunofluorescent staining (red) and neutrophils with typical NET morphology (right panel, scale bar 40μm). Blue = nucleus. Grey = actin. **(E)** Infiltrating macrophages infiltrate the livers of STAM mice at a later time point (8 weeks) than neutrophils, concurrent with an increase in the serum level of IL-6 **(F)**.

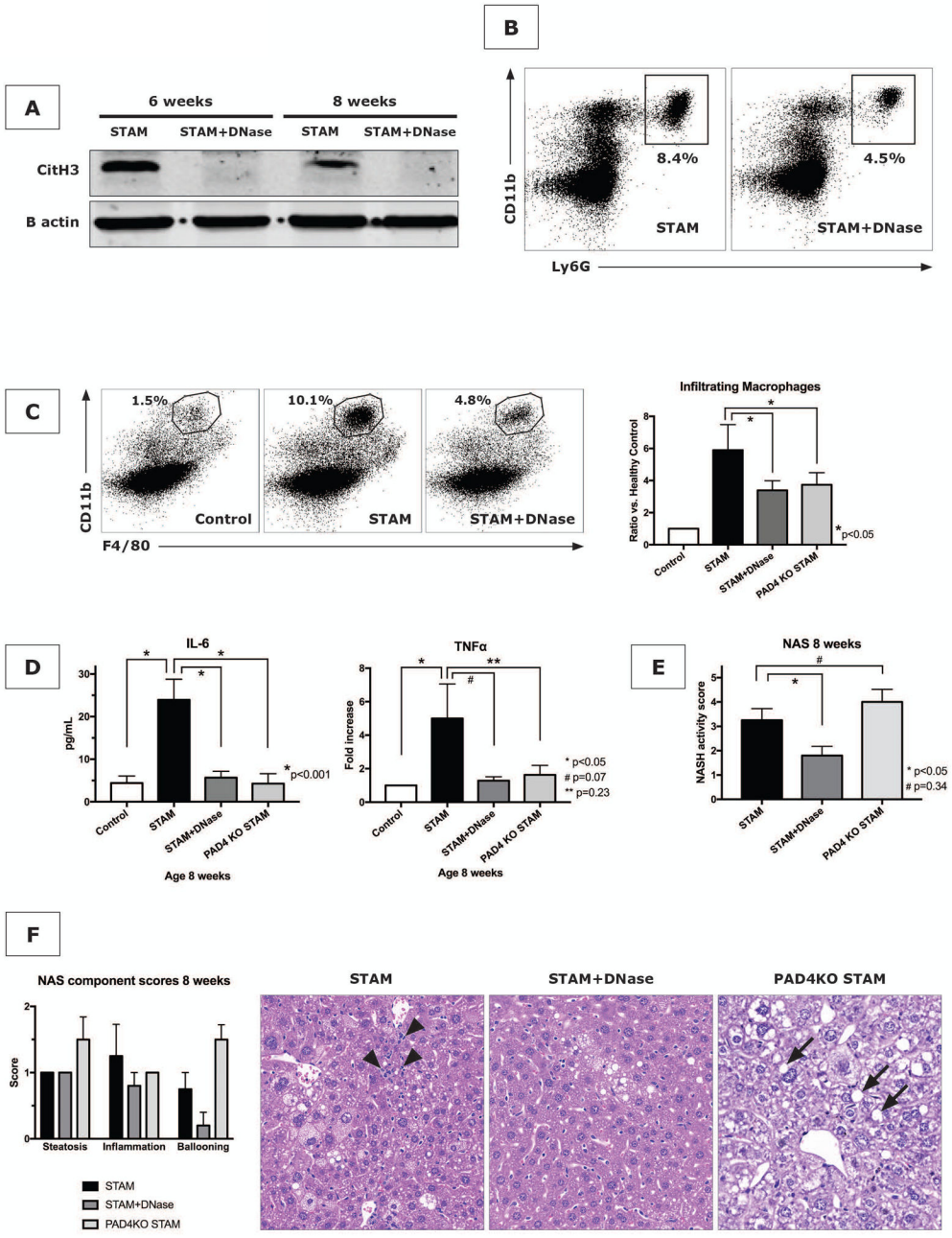

Figure 4. NET inhibition reduces macrophage infiltration, inflammatory cytokines, and NASH

(A) DNase treatment reduces liver CitH3 expression in STAM mice. (**B**) NET blockade with DNase in STAM mice reduces further neutrophil infiltration as shown for 8 weeks. Both DNase and PAD4$^{-/-}$ reduced several hallmarks of NASH including macrophage infiltration (n=4 mice per group) (**C**) and production of inflammatory cytokines IL-6 and TNF-α (n=8 mice per group) (**D**). NASH activity scores (n=5 mice per group) (**E**), with a reduction of inflammation, but unaffected presence of liver fat (**F**). H&E stained liver of STAM mice with lobular inflammation (arrow heads), which was improved by DNase treatment and in

PAD4$^{-/-}$ mice, although PAD4$^{-/-}$ livers demonstrated accelerated development of steatosis (arrows) (**F**). (all shown for time point 8 weeks).

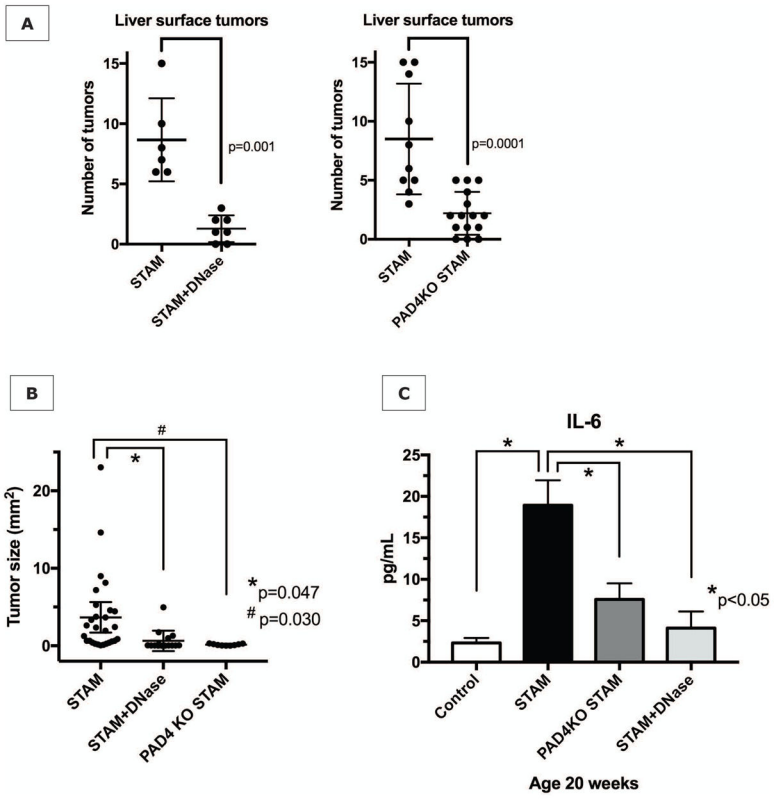

Figure 5. NET inhibition reduces progression of NASH to HCC

(A) NET inhibition for 20 weeks with daily DNase treatment, or by gene knockout for peptidylarginine deaminase (PAD4KO) significant reduces tumor formation at 20 weeks. **(B)** Tumor size analysis of the largest 3 tumors found at a random section through the liver revealed significantly reduced tumor sizes in DNase-treated mice and PAD4$^{-/-}$ mice, compared to untreated wild type STAM mice. **(C)** Serum IL-6 levels remain decreased, suggesting that NET inhibition persistently alters the inflammatory environment in which HCC arises.

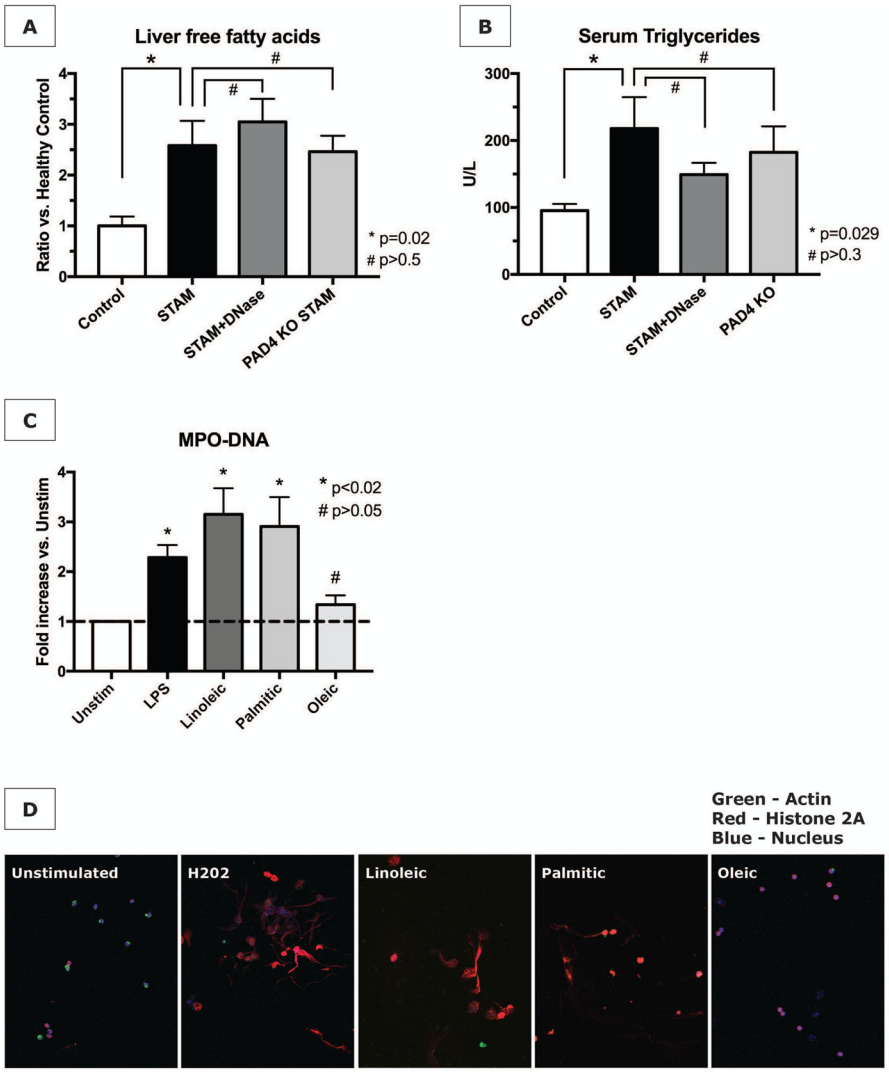

Figure 6. Free fatty acids stimulate NET formation in vitro

(A) Livers from STAM mice have increased levels of free fatty acids (FFA). NET inhibition does not prevent the increase in FFA. **(B)** NET abrogation also does not prevent elevated serum triglycerides. **(C)** Isolated neutrophils were stimulated with LPS as positive control, or with various FFA at 50nM for 4h. MPO-DNA complexes in culture supernatants were significantly elevated after stimulation with linoleic and palmitic acid (data represent n=4 independent experiments per group). **(D)** Immunofluorescent staining for NETs was concordant with supernatant MPO-DNA levels.